

Minimization of Optical Rogue Waves Formation Based on Hamiltonian Approach

Hugo Wai Leung MAK

Department of Mathematics, The Hong Kong University of Science and Technology, Clearwater Bay, Kowloon,
Hong Kong

hwlmak@ust.hk

Abstract

It is well known that Benjamin-Feir instability plays a crucial role in generating underseas rogue waves, for which its formation process can be carried out within a short period of time, but causing devastating threats to our natural habitats. One can attempt to control or stabilize such nonlinear plane waves via self-dissipation, provided that amplitude of such waves is sufficiently low. For rogue waves with higher amplitude, it suffices to observe the stable wave patterns underseas, and makes use of damping techniques to recover its original amplitude into normal amplitudes. Currently, there is a lack of specialized mathematical tools for analyzing underlying physics of these large magnitude nonlinear rogue waves. In this paper, we provide a framework of mathematical model for formation of rogue waves, and demonstrate statistical properties of optical rogue waves through Hamiltonian approach (that is widely used in statistical mechanics field). Next, we formulate new optimization criteria for minimizing its intensity by making use of first-order Riccati differential equation, and outline several important physical factors that we need to control in reality. This opens a new door for mitigating detrimental effects from fiber nonlinearity in optical communications.

Keywords: Rogue Waves, Nonlinear Optics, Statistical Mechanics (Hamiltonian), Benjamin-Feir Instability

I. Introduction

Rogue waves, also known as "killer waves," are rare events of high-intensity fluctuations occurring in oceans and in communication links. These waves are also ubiquitous in various fields ranging from optics to acoustics and hydrodynamics. Though confirmation of rogue wave events took place in 1995, such concept was applied into nonlinear-optical-fiber-based systems in 2007 [1]. Nowadays, it is widely applied into supercontinuum generation in fibers and optical turbulence. The initial and fundamental mechanism of formation of rogue waves is called modulation instability (MI) [2]. Energy transfer takes place during the process, and it is built up through an "almost" resonant Four-Wave Mixing (FWM) process. We first investigate analytical solutions satisfying the 1D Nonlinear Schrödinger Equation (NLSE), which represents prototypes of rogue waves. After obtaining a close form of these solutions, we (i) propose to apply Hamiltonian concept in statistical physics to describe properties of rogue waves, (ii) formulate an optimization problem in minimizing intensity of rogue waves through isospectral deformation of Hamiltonian function, (iii) solve the problem for some given parameter values, and (iv) attempt simulation to do analysis of rogue wave formation and to reduce intensity of rogue waves. To our best knowledge, this is the first time of adopting Hamiltonian approach from statistical physics to govern dynamics of rogue waves, such new formulation provides a systematic way to reduce rogue wave intensity, which can be applied to space division multiplexed (SDM) transmission and modulated laser injection.

II. Principles & Mathematical Model of Formation of Rogue Waves

In 1967, Benjamin and Feir verified that a uniform periodic wavetrain possessing moderate and finite amplitude underseas is unstable to infinitesimal perturbations [3]. Such instability is in analogy with growing modulation of a plane wave, in which the process amplifies slight periodic perturbation into formation of high intensity pulse trains during evolution, and is known as Modulation Instability (MI) in the literature. Figure 1 provides a simple analogy of MI, where two waves with slight difference in frequency travel in opposite

direction, i.e. towards each other (Figure 1(a)), and they superpose to form a resultant waveform with amplitude doubled at a particular position, $z = 40$ m (Figure 1(b)).

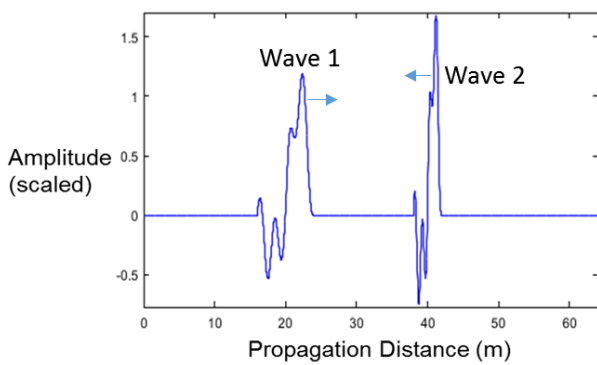


Figure 1(a)

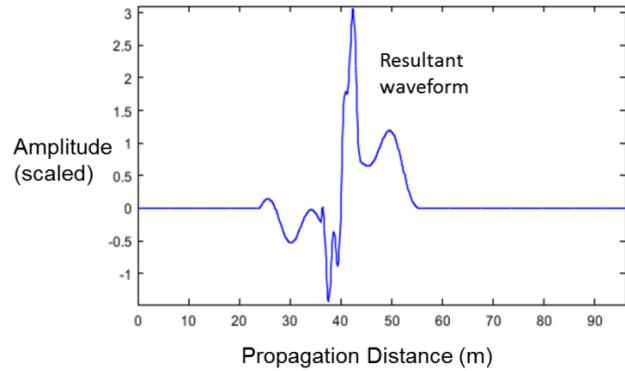


Figure 1(b)

Figure 1. An analogy showing formation of rogue wave at a specific location

Figure 1(a). Two waveforms (Wave 1 and Wave 2) with slight difference in frequency propagate in opposite direction (with Wave 1 to the right and Wave 2 to the left)

Figure 1(b). Resultant waveform when Wave 1 and 2 superpose, and the peak wave amplitude becomes doubled at a specific location, namely $z = 40$ m.

One possible mathematical model to describe rogue waves is to make use of rational solutions of the NLSE, but in general, the possible prototypes of rogue waves are the analytical solutions to the integrable 1D focusing NLSE and defocusing NLSE, as shown in (1) and (2) respectively. Bright soliton solutions are found in (1), while (2) contains all dark soliton solutions.

$$i \frac{\partial u}{\partial t} + \frac{\partial^2 u}{\partial z^2} + \frac{1}{2}|u|^2 u = 0 \tag{1}$$

$$i \frac{\partial u}{\partial t} + \frac{\partial^2 u}{\partial z^2} - \frac{1}{2}|u|^2 u = 0 \tag{2}$$

Here u denotes the wave envelope, t as the temporal variable and z as the spatial variable in the frame moving with rogue waves. Some examples of analytical solutions satisfying (1) are Akhmediev breather (with attenuation factor of 0.25) and Peregrine soliton (with attenuation factor of 0.5). The general form of solutions

of (2) is rational and oscillatory, and is in the form of $u(z, t) = \frac{x(z, t)}{y(z, t)} \left[\cos\left(\frac{-z^2}{6t}\right) + i \sin\left(\frac{-z^2}{6t}\right) \right]$, where $x(z, t)$

and $y(z, t)$ are z and t dependent polynomials. Such class of solutions is known as “generalized Okamoto polynomials”, which are rational solutions of the 4th Painlevé equation obtained by performing inverse scattering to (2). More details can be found in [4]. Substituting the roots of rational solutions of (2) to (1),

rational solutions to (1) can be expressed in the form of $u_1(z, t) = \frac{x_1(z, t)}{y_1(z, t)} \left[\cos\left(\frac{t}{2}\right) + i \sin\left(\frac{t}{2}\right) \right]$.

Here we assume $y_1(z, t)$ to be real and positive for every real values of z and t such that the waveform is well-defined at all points.

III. Statistical Properties of Rogue Waves in Optical Fibers

In previous sections, we showed that solitons are exact complex differentiable solutions of NLSE, and generation of an extreme high intensity soliton at fiber output port will cause irregular events, leading to perturbation of optical signals to be transmitted. Therefore, understanding reasons of formation of extreme amplitude peaks due to rogue waves are particularly important. Traditionally, researchers make use of several quantities like eigenvalues and amplitudes of wavefunction and attenuation factors for analysis. Instead of using classical approach, we propose a new method and formulation in this paper, which is to investigate statistical properties of rogue waves through Hamiltonian concept in statistical physics. Such concept is applicable to all fields and phenomenon without any restrictions, provided that we can formulate the total energy possessed by the system. Classically, N atomic spins are arranged as a lattice with each spin interacting with neighboring spins. In the absence of external magnetic field, Hamiltonian is shown in (3), where σ_A denotes the spin at site A (+1 or -1), B includes set of all nearest neighbor sites of site A and J_{AB} is the realization of coupling of Gaussian distribution, while $1/\sqrt{N}$ acts as a re-scaling factor.

$$H_{J,N} = \frac{-1}{\sqrt{N}} \sum_{1 \leq A < B \leq N} J_{AB} \sigma_A \sigma_B \quad (3)$$

We formulate a similar Hamiltonian system to govern the weak interactions between fiber solitons by considering a slightly different 1D NLSE with third-order dispersion effects as shown in Equation (4), with u, z, t defined similarly as in (1) and (2), and σ represents normalized third-order dispersion coefficient.

$$i \frac{\partial u}{\partial z} + \frac{1}{2} \frac{\partial^2 u}{\partial t^2} + |u|^2 u - i\sigma \frac{\partial^3 u}{\partial t^3} = 0 \quad (4)$$

Equation (4) is now no longer integrable, so we cannot verify the existence of analytic solutions. However there are several statistical quantities defined: Normalized power of the optical fiber system $P = \int |u(t)|^2 dt$, total momentum of the optical fiber system $M = \int \omega |u(\omega)|^2 d\omega$, with ω as the angular frequency, and Hamiltonian of the optical system as H . In terms of above parameters, Hamiltonian of system is expressed as the summation of linear (time-independent) dispersive contribution (H_L) and nonlinear contribution (H_{NL}) in (5) (See [5] and [6]).

$$H = H_L + H_{NL} = \int \left(\frac{\omega^2}{2} - \sigma\omega \right) |u(\omega)|^2 d\omega + \int -\frac{1}{2} |u(t)|^4 dt \quad (5)$$

Though (4) is nonlinear, quasi-soliton solutions exist based on (5) by building up an energy profile, by which we know clearly the exact position where a rogue soliton is generated. To determine the position is equivalent to the construction of an Hamiltonian landscape profile that shows weak interactions of nonlinear Schrödinger solitons, and the deep minimum (but NOT shallow minimums) of Hamiltonian profile represents the position where a rogue soliton is generated at optical fiber output. When the Hamiltonian term reaches its minimum, corresponding intensity reaches peaks. In undersea environment, apart from considering MI, perturbation of velocity potential and free surface elevation of Stokes waves should be taken into consideration for obtaining third order solutions representing nonlinearities. Using Hamiltonian approach, 1D NLSE is converted into the form of (6), where A_0 represents spatial and time dependent wave amplitude, k, c and ω are corresponding to wavenumbers, speed of light and angular frequency of carrier wave, respectively, and $\delta(z, t)$ denotes the surface elevation.

$$\begin{cases} i \left(\frac{\partial A_0}{\partial t} + c \frac{\partial A_0}{\partial z} \right) = \frac{\omega}{8k^2} \frac{\partial^2 A_0}{\partial z^2} + \frac{\omega k^2}{2} |A_0|^2 A_0 \\ \delta(z,t) = \frac{1}{2} \left(A_0(z,t) e^{i(kz - \omega t)} + c.c. + \dots \right) \end{cases} \quad (6)$$

In optical fibers, the dynamical process that gives rise to extreme amplitude peaks at fiber outputs can be explained with respect to Hamiltonian concept. A sequence of minor collisions occurs within optical fiber, and each collision corresponds to minimization of interacting Hamiltonian between two neighboring solitons. To compute the resultant Hamiltonian, it suffices to integrate the nonlinear terms of Hamiltonian density H_D , which is the sum of kinetic energy density T_D and potential energy density V_D . Throughout the process, minor collisions create numerous small peaks, but the one happening at fiber output will lead to formation of a sharp peak in intensity, thus supercontinuum generation is resulted. Numerical root finding techniques like method of bisection or Newton's method can be further applied to analyze the stability and convergence of equilibrium points.

IV. Criteria of Minimization of Rogue Waves

In previous sections, we understand that if amplitude of optical pulses is not effectively controlled, formation of rogue waves may cause devastating optical damage to data transmission through fibers or optically injected lasers. Our goal is to minimize intensity of optical rogue waves. It is known that the dimensionless equation governing rogue wave dynamics possesses wide class of self-similar solutions, in which it assumes the refractive index (n) of the nonlinear fiber amplifier to be $n = n_0 + n_1 F(z)x^2 + n_2 |E|^2$, where $n_1 > 0$ and n_2 represents the defocusing parameter and Kerr nonlinearity, $F(Z)$ denotes the tapering potential function in optical fibers and $E(x, z)$ is the complex envelope of spatial dependent electric field. In addition, we define $W(z)$ as the similariton width. Next, adopting a fact in quantum mechanics to apply isospectral deformation of Hamiltonian for a given ground state wavefunction and energy, we obtain time-dependent Hamiltonian

$$H \left(\frac{t}{t_0} \right) = e^{\frac{xt}{t_0}} \cdot H_0 e^{-\frac{xt}{t_0}} \quad \text{with } 0 \leq t \leq t_0.$$

The remaining task is to select an appropriate x such that x itself is an anti-Hermitian operator, and at the time instant $t = t_0$, the Hamiltonian function returns to initial state. This will result in a class of tapering functions ($\bar{F}(Z)$) and similariton widths ($\bar{W}(Z)$), where $Z = z/L_D$ and L_D denotes the diffraction length. One traditional example is given in [7], as shown in (7), where R denotes the Riccati parameter satisfying first-order Riccati differential equation of the form $R'(z) = A(z) + B(z)R(z) + C(z)R^2(z)$, with A, B and C as arbitrary functions depending on x .

$$\bar{F}(Z) = F(Z) - 2 \frac{d}{dZ} \left(\frac{W(Z)}{R + \int_{-\infty}^Z W^2(S) dS} \right), \quad \bar{W}(Z) = \left(\frac{\sqrt{R^2 + R}}{R + \int_{-\infty}^Z W^2(S) dS} \right) W(Z) \quad (7)$$

As a numerical example, taking $W(Z) = \text{sech } Z$, we construct and compare the graphs of $\bar{W}(Z)$ with $W(Z)$ by varying R from 0.1 to 10 in Figure 2. It is noticed that when the Riccati parameter R increases, the profile assembles itself with actual functions and approaches asymptotic values when R is sufficiently large.

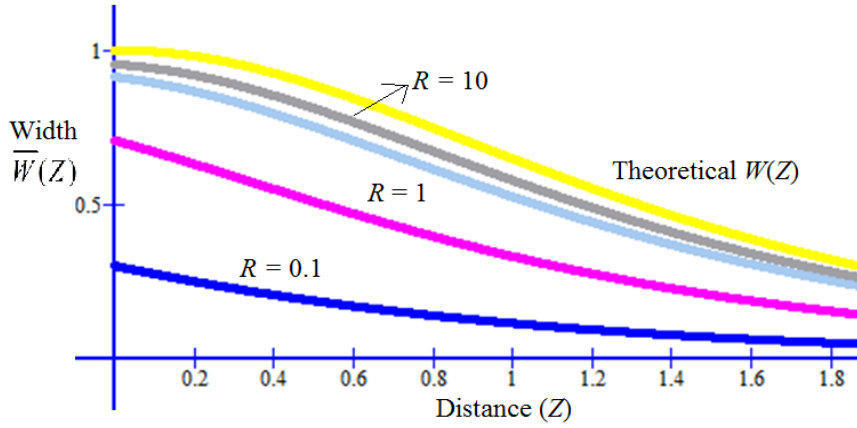


Figure 2. Profiles of sech Z (yellow curve) and similariton widths $\bar{W}(Z)$ with $R = 0.1, 1, 5, 10$ (blue, purple, light blue and grey curves)

with respect to distance (Z)

Next, we formulate an optimization problem as follows. Notice that first-order intensity (I_1) and second-order intensity (I_2) are inversely proportional to square of $W(Z)$, therefore minimizing intensity of optical rogue waves is equivalent to the following:

$$\min I_k(Z) \text{ for } k = 1,2 \Leftrightarrow \begin{cases} \max R(x) \dots \dots \dots (8.1) \\ \text{subject to } R'(z) = A(z) + B(z)R(z) + C(z)R^2(z) \dots \dots \dots (8.2) \\ \bar{W}(Z) \text{ and } \bar{F}(Z) \text{ are maximized. } \dots \dots \dots (8.3) \end{cases} \quad (8)$$

For simplicity, we may assume $A(z) = 0$ and $B(z) = C(z) = 1$, solving (8.2) in particular, we obtain $z = \log\left(\frac{R(z)}{R(z)+1}\right)$ by setting the additive constant to be 0.

From (7) and (8.3), we obtain the necessary criteria shown in (9):

$$\frac{d^2}{dZ^2} \left(\frac{W(Z)}{R + \int_{-\infty}^Z W^2(S)dS} \right) = \frac{F'(Z)}{2} \dots \dots \dots (9.1)$$

$$\frac{W'(Z)}{W(Z)} = -\frac{\frac{d}{dZ} A(Z)}{A(Z)}, \text{ where } A(Z) = \frac{\sqrt{R^2 + R}}{R + \int_{-\infty}^Z W^2(S)dS} \dots \dots \dots (9.2)$$

(9)

$$\log\left(\frac{R(L_D Z)}{R(L_D Z)+1}\right)$$

For this particular case, we plug back $Z = \frac{\log\left(\frac{R(L_D Z)}{R(L_D Z)+1}\right)}{L_D}$ into (9) and carry out the corresponding differential operations. This particular result successfully minimizes the intensity of optical rogue waves in (8). This formulation can be generalized into solving (8) completely, and the set of roots of Z exactly represent the minimum points in the graph of Hamiltonian versus position. Knowing all these information, it suffices to control formation of rogue waves at these specific locations by alternating modulation frequencies, which alleviates devastating effects due to rogue waves.

V. Numerical Results and Simulations

In previous section, we discuss the mathematical formulation and statistical properties of rogue waves, so how should we identify its positions of occurrence and relate it to Hamiltonian concepts?

In literature (in Section 2 of both [8] and [9]), a pulse is considered as rogue wave if its intensity exceeds the preset intensity threshold I_t , where $I_t = \bar{I} + 6\sigma$. Here \bar{I} represents the mean intensity of waveform and σ indicates the corresponding standard deviation. In the sketch of relative intensity versus position, as shown in Figure 3, rogue wave can be found exactly in position X, since its relative intensity is larger than the intensity threshold. The sketch is an analogy to data transmission occurring in optical fibers. We may assume $z = 0$ as the opening end of optical fiber, where data goes in and is transmitted. We can identify the exact position (X) where rogue waves may occur during data transmission that will certainly hinder the process and alter the information to be transmitted. This is a crucial step that we should attempt before finding ways of controlling rogue wave formation.

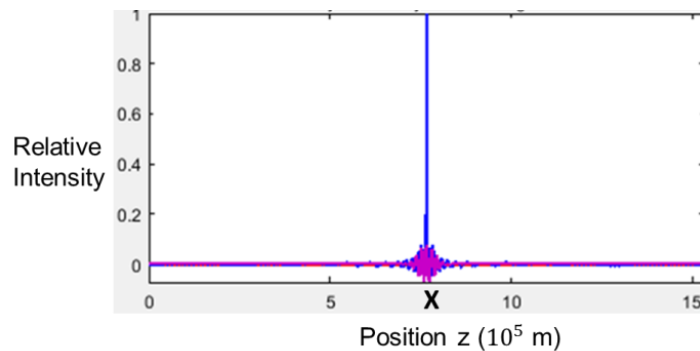


Figure 3. An analogy of occurrence of rogue wave patterns – Sketch of Relative Intensity (Scaled) with respect to position (from 0 to 15×10^5 m)

Though Figure 3 shows the appropriate analogy of formation and detection of rogue wave at a particular position, transmitted signals via optical fibers are not as smooth as what is shown in Figure 3 due to several factors, including nonlinear distortion and crosstalk, noises induced in both input optical pulses and surrounding environment inside the optical fiber and fiber dispersion effects. All these factors impose nonlinearities onto the fiber, thus increase the complexity of the transmitted signal in reality, where there may be huge fluctuation in intensity when frequency or wavelength is altered slightly.

Figure 4 is an example of the distorted signal occurred in real life circumstances. We use the same criteria for identification of rogue waves. At frequency of 2500 Hz, the relative intensity exceeds the intensity threshold I_t , so rogue waves are formed at this particular frequency. However, though there are peaks situating at frequency of 2650 Hz and 3450 Hz and local maximum occurring at frequency of 1550 Hz, these wave patterns are not considered as rogue waves, since its relative intensity does not exceed I_t . Previous literature has

proposed to identify the frequency of rogue wave formation, then add low-energy wavepackets to alter statistics of soliton amplitude [10]. Therefore, collection of relative intensity level at different frequency is vital.

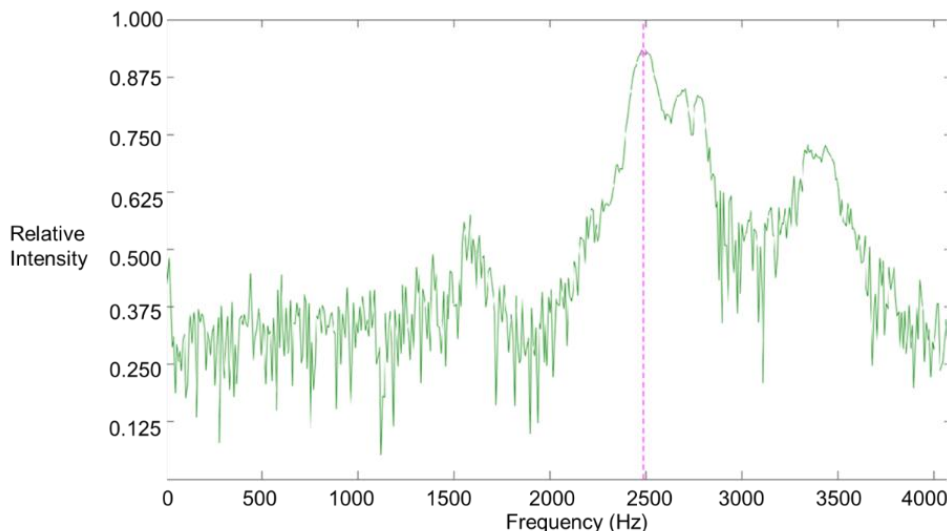


Figure 4. Sketch of relative intensity at different frequencies of a distorted signal in daily lives, where rogue waves are formed at 2500 Hz

From our discussion in Section III, there is an alternative way of identifying rogue soliton in optical transmission, that is to look for the deep minimum in a Hamiltonian profile. Figure 5 shows an example of Hamiltonian profile, where a deep minimum is found at frequency of 2200 Hz. This implies that the corresponding intensity reaches peak at this particular frequency, in which frequency modulation or injection of wavepackets should be adopted to avoid formation of rogue waves, which hinders the progress of data transmission.

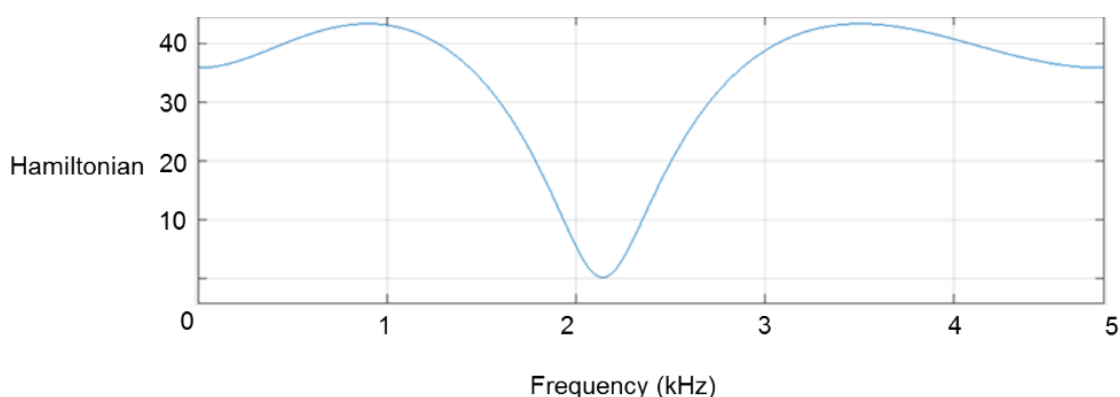


Figure 5. An example of Hamiltonian profile at different frequencies, where formation of rogue soliton is indicated by presence of troughs

The aforementioned implication can be further noticed from construction of Hamiltonian profile and relative intensity graph at different wavelengths. As shown in Figure 6(a), the waveform is the combination of hyperbolic secant curve together with induced input pulse noise, which is a demonstration of the distorted signal occurring in our daily lives, especially in the field of optical transmission. A major peak is observed at

around 1060 nm, and several minor peaks are observed due to fluctuation of signals and effect induced by the noise content. It is certain that a rogue soliton is generated at 1060 nm, but for other wavelengths, we are uncertain whether the small peaks in relative intensity are due to formation of rogue soliton at fiber output, or it simply represents the effect of noise, or even other external factors. Therefore, for the purpose of verification, we look closely to the density plot of Hamiltonian of spectral evolution for a rare event that will lead to formation of rogue solitons. Figure 6(b) shows Hamiltonian distribution at different wavelengths, ranging from 1010 nm to 1170 nm. Such range is set and investigated based on the major peaks found and detected in Figure 6(a). It is obvious that a deep minimum occurs at 1060 nm, which further verifies the occurrence of rogue soliton at this particular wavelength.

Next, from Figure 6(a), we suspect that rogue solitons are also formed at other wavelengths, where the relative intensity looks high and minor peaks are formed. In order to detect rogue soliton accurately, it suffices to refer to Figure 6(b). A relatively shallow minimum at 1110 nm indicates another rare event leading to another rogue soliton, though the Hamiltonian of this soliton is higher than the one generated at 1060 nm. Usually, Hamiltonian of a system consists of the linear dispersive and nonlinear contribution (See (5) in Section III), further investigation is needed to identify the origin that causes the difference in Hamiltonian.

From the deduction of Figure 6(a) and Figure 6(b), one expects that making use of Hamiltonian profile has a much higher accuracy in identification of rogue waves comparing with intensity profile. Obviously, a clear peak is obtained in Figure 6(a), however there are several more small peaks, and we are uncertain which of them represent occurrence of rare events, therefore we cannot come to an accurate and definite conclusion. One needs to rely on finding the deep minimums of Hamiltonian profile, as shown in Figure 6(b), the density plot makes everything much clearer and one may spot out the significant turning points immediately.

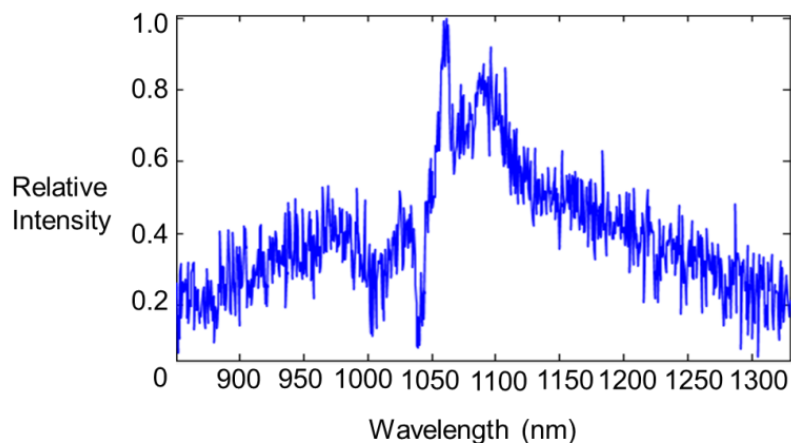


Figure 6(a). Sketch of intensity at different wavelengths for a Hyperbolic secant input signal together with induced noise

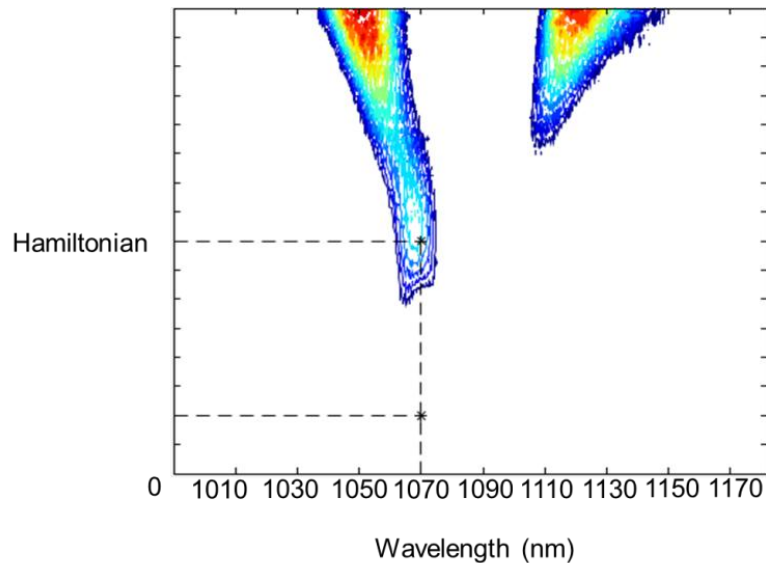


Figure 6(b). Hamiltonian profile of spectral evolution of rogue wave events at specific wavelengths, namely 1065 nm and 1110 nm

After accurate identification of positions or specific wavelengths for rogue solitons to be generated, the next step is to think of suitable methods to harness or reduce the detrimental effects caused by rogue waves.

VI. Discussion – Minimization of Optical Rogue Waves Formation in Reality

In previous sections, we describe the mathematical approach and formulation for minimization of optical rogue waves, and provide some numerical results for identification of rogue waves. But in reality, how to control the formation of optical rogue wave is still an open problem, since occurrence of rogue wave events is only formulated in statistical relation, but not in definite mathematical terms, so we can only give a prediction for its occurrence and estimate the position where these optical rogue waves are formed.

In previous sections, together with [7], when the Riccati parameter, a free parameter to the first order Riccati differential equation, as listed in Equation (8.2) is larger, the amplitude of rogue waves reach its asymptotic values, as well as its tapering width. This indicates that the intensity of rogue waves or any common underwater waves will be lowered when Riccati parameter becomes larger. This phenomenon can be observed from both first-order intensity and second-order intensity of wavetrains. Therefore, one practical way of controlling amplitude of rogue waves is to make Riccati parameter larger. In practice, the Riccati parameter cannot reach an infinite value, since it is based on the physical properties of optical fibers or transmission link itself, therefore engineers should always aim at designing and adopting suitable transmission fibers underseas, thus creating an opportunity for harnessing formation of rogue wave patterns.

The techniques of fiber design and formulation were well investigated recently by Dudley *et al.* [11] and Zhao *et al.* [12]. Dudley *et al.* have demonstrated the enhancement or harnessing of rogue wave intensity and burst of localized noise on pulse leading edges [11], while Zhao *et al.* verified numerically that rogue waves intensity can be hugely reduced with the use of cascaded photonic crystal fiber, as it can generate supercontinuum with broader and smoother wave spectrum [12]. Further numerical simulations can be conducted with the help of data assimilation techniques (as suggested in [13]), by setting the results in [12] as initial input of the physical system governed by differential equations described in Section IV of this paper.

Moreover, the initial input optical pulses moving into the optical fiber itself produce significant noises and perturbations to the signals or information to be transmitted, and such pulses are coming from all directions and with varying intensities in underseas environment, so it is hard to measure or even harness its formation.

Such noises are also directly related to the nonlinear damping coefficient and fiber dispersion effects occurring within the fiber. To minimize formation of optical rogue waves in reality, one should examine the performance of the fiber based on different input noise intensity or characteristics. Yoon *et al.* has provided us a clue to adopt an explicit data assimilation scheme to predict formation of nonlinear waves with the help of explicit Kalman filter [14]. One may extend the investigation by analyzing the statistical fluctuation of position due to random noise or slight perturbations.

We demonstrate a statistical framework for analysis as follows. The wave profile in appearance can be denoted by $\tilde{P}(t)$, and can be decomposed into two parts, $P(t)$ and $\delta P(t)$ respectively. Here $P(t)$ represents the true spatial and time dependent wave profile, and $\delta P(t)$ represents the stationary deviation caused by noises or external perturbations. Using simple statistics, one can verify that $\langle \delta P(t), \delta P(t') \rangle = 0$ if t is not equal to t' , $\langle \delta P(t) \rangle = 0$ and $\langle \delta P^2(t) \rangle = \varepsilon^2$, where ε stands for the spatial resolution of wave. Apart from static errors formulated above, there are dynamic errors caused by continuous movement of rogue wave patterns. We assume the acquisition time by continuous movement to be δt , then the spatial rogue wave pattern obtained at time t $\bar{P}(t, \delta t)$ consists of mixture of all rogue wave profiles within $[t - \delta t, t]$, and can be described by the integral in (10).

$$\bar{P}(t, \delta t) = \frac{1}{\delta t} \int_0^{\delta t} P(t - \tau) d\tau \quad (10)$$

The integral in (10) consists of some errors that cannot be reduced via all means of adjustments.

The above statistical framework formulation helps to classify the potential errors into two kinds, static errors and dynamic errors respectively. In order to harness the intensity of rogue waves, one should target at reducing static errors, which are normally caused by noise, perturbations and discrepancies in spatial resolution. This indirectly reduces the probability for optical rogue wave formation.

VI. Conclusion

In this paper, we successfully demonstrate statistical properties of formation of rogue waves through Hamiltonian approach and Benjamin-Feir instability, which shows the combination of statistical physics and photonics in solving real life problems in the field of nonlinear optics. Then, we solve the formulated optimization problem to minimize rogue wave intensities, under several mathematical assumptions and substitutions. We also carry out numerical simulations to verify that positions or regions with highest wave intensity (which are classified as rogue waves or "killer" waves) underseas will have lowest Hamiltonian, here Hamiltonian of our system is expressed as summation of linear (time-independent) dispersive contribution and nonlinear contribution. In our simulation, spectral evolution of rogue wave events take place at specific wavelengths, namely 1065 nm and 1110 nm respectively. In reality, rogue wave events may take place in more wavelengths values, which increase the difficulties in predicting exact time of its formation. Therefore, there is a need to control some physical parameters in optical fibers or within the transmission links. We summarized several such possible ways mentioned in previous literature, which includes increasing Riccati parameter, use of cascaded photonic crystal fiber, Kalman filters and data assimilation techniques based on existing trends and occurrence of rogue wave events. We also provided a statistical analysis of fluctuation of wave patterns caused by injection of random noise and perturbations, and subdivided respective errors into two types: static errors and dynamic errors. In overall, clear understanding of formation of rogue wave patterns is crucial, as it implicates a possibility for engineers and scientists to alleviate detrimental effects caused by rogue wave events. The approach adopted in this paper can be applied to many communication aspects, for example signal transmission processes and bit-overlapping transmission in fiber communications links.

Data availability. No data sets were used in this article.

Competing interests. The author declare that they have no conflict of interest.

Acknowledgements. The author gratefully acknowledge supports and encouragements from Prof. Lian Kuan CHEN, Department of Information Engineering, The Chinese University of Hong Kong.

References.

1. D. R. Solli, C. Ropers, P. Koonath, and B. Jalali, "Optical rogue waves", *Nature*, 450, pp. 1054-1057, Dec 2007, <https://www.nature.com/articles/nature06402>
2. S. Trillo, S. Wabnitz, "Dynamics of the nonlinear modulational instability in optical fibers", *Optics Letters*, Vol. 16, No. 13, pp. 986-988, July 1991, <https://www.osapublishing.org/abstract.cfm?uri=ol-16-13-986>
3. T. B. Benjamin, J. E. Feir, "The disintegration of wavetrains in deep water", Part 1, *J. Fluid Mech.*, 27, pp. 417-430, 1967, <https://www.cambridge.org/core/services/aop.../S002211206700045X>
4. P. Bassom, P. A. Clarkson, A. C. Hicks and J. B. McLeod, "Integral Equations and Exact Solutions for the Fourth Painleve Equation", *Mathematical and Physical Sciences*, vol. 437, No. 1899, pp. 1 – 24, Apr 1992, <http://rspa.royalsocietypublishing.org/content/royprsa/437/1899/1.full.pdf>
- A. Armaroli, C. Conti and F. Biancalana, "Rogue solitons in optical fibers: a dynamical process in a complex energy landscape?", *Optica*, Vol. 2, No. 5, pp. 497 – 504, May 2015, <https://www.osapublishing.org/abstract.cfm?uri=optica-2-5-497>
5. F. Biancalana, A. Armaroli, and C. Conti, "Unified explanation for rogue waves in optical fibers", *Spie, Optoelectronics and Communications*, pp. 1 – 4 , 2015, <http://spie.org/newsroom/6035-unified-explanation-for-rogue-waves-in-optical-fibers?SSO=1>
6. C. N. Kumar *et al.*, "Controlled giant rogue waves in nonlinear fiber optics", *Physical Review A* 86, 025802, pp. 1 – 5, Aug 2012, <http://link.aps.org/doi/10.1103/PhysRevA.86.025802>
7. J. Ahuja, D. B. Nalawade, J. Z-Munt, R. Vilaseca and C. Masoller, "Rogue waves in injected semiconductor lasers with current modulation: role of the modulation phase", *Optics Express*, Vol. 22, No. 23, pp. 1 – 6, Nov 2014, <https://www.osapublishing.org/abstract.cfm?uri=oe-22-23-28377>
8. S. Perrone, R. Vilaseca, J. Z-Munt and C. Masoller, "Controlling the likelihood of rogue waves in an optically injected semiconductor laser via direct current modulation", *Physical Review A* 89, pp. 1 – 6, 2014, <https://link.aps.org/doi/10.1103/PhysRevA.89.033804>
- A. Demircan, Sh. Amiranashvili, C. Bree, F. Mitschke and G. Steinmeyer, "Rogue wave buster", *QW3E.1, CLEO* 2013, <http://ieeexplore.ieee.org/iel7/6820093/6832912/06834562.pdf>
9. John. M. Dudley, Goëry Genty, and Benjamin J. Eggleton, "Harnessing and control of optical rogue waves in supercontinuum generation", *Optics Express* Vol. 16, Issue 6, pp. 3644-3651 (2008), <https://www.osapublishing.org/abstract.cfm?uri=oe-16-6-3644>
10. Saili Zhao, Hua Yang, Chujun Zhao, and Yuzhe Xiao, "Harnessing rogue wave for supercontinuum generation in cascaded photonic crystal fiber", *Optics Express* Vol. 25, Issue 7, pp. 7192-7202 (2017), <https://www.osapublishing.org/abstract.cfm?uri=oe-25-7-7192>

11. Jean-Michel Lefèvre and Lotfi Aouf, "Latest developments in wave data assimilation", ECMWF Workshop on Ocean Waves, 25-27 June 2012, <https://www.ecmwf.int/sites/default/files/elibrary/2012/10699-latest-developments-wave-data-assimilation.pdf>
12. Seongjin Yoon, Jinwhan Kim, Wooyoung Choi, "An Explicit Data Assimilation Scheme for a Nonlinear Wave Prediction Model Based on a Pseudo-Spectral Method", IEEE Journal of Oceanic Engineering, Vol. 41, Issue 1, pp. 112 – 122 (2016), <http://ieeexplore.ieee.org/document/7055936/>